Available online at www.sciencedirect.com
ScienceDirect
Dyes and Pigments 75 (2007) 701–713
DYES and PIGMENTS
www.elsevier.com/locate/dyepig

Adsorption kinetics and mechanism of cationic methyl violet and methylene blue dyes onto sepiolite

Mehmet Doğan*, Yasemin Özdemir, Mahir Alkan

Balikesir University, Faculty of Science and Literature, Department of Chemistry, 10100 Balikesir, Turkey

Received 19 February 2006; received in revised form 12 April 2006; accepted 25 July 2006
Available online 27 October 2006

Abstract

The use of low-cost and ecofriendly adsorbents was investigated as an ideal alternative to the current expensive methods of removing dyes from wastewater. Sepiolite was used as an adsorbent for the removal of methyl violet (MV) and methylene blue (MB) from aqueous solutions. The rate of adsorption was investigated under various parameters such as contact time, stirring speed, ionic strength, pH and temperature for the removal of these dyes. Kinetic study showed that the adsorption of dyes on sepiolite was a gradual process. Quasi-equilibrium reached within 3 h. Adsorption rate increased with the increase in ionic strength, pH and temperature. Pseudo-first-order, the Elvoich equation, pseudo-second-order, mass transfer and intra-particle diffusion models were used to fit the experimental data. The sorption kinetics of MV and MB onto sepiolite was described by the pseudo-second-order kinetic equation. Intra-particle diffusion process was identified as the main mechanism controlling the rate of the dye sorption. The diffusion coefficient, D, was found to increase when the ionic strength, pH and temperature were raised. Thermodynamic activation parameters such as ΔG^*, ΔS^* and ΔH^* were also calculated.
© 2006 Elsevier Ltd. All rights reserved.

Keywords: Sepiolite; Dyes; Adsorption; Adsorption kinetics; Diffusion; Activation parameters

1. Introduction

Color effluents have been produced ever since the dyeing technique was invented. Various kinds of synthetic dyestuffs appear in the effluents of wastewater in various industries such as dyestuff, textiles, leather, paper. Concern exists since a very small amount of dye in water is highly visible and may be toxic to aquatic creatures [14]. The removal of color synthetic organic dyestuff from waste effluents becomes environmentally important. It is rather difficult to treat dye effluents because of their synthetic origins and their mainly aromatic structures, which are biologically non-degradable. Among several chemical and physical methods, adsorption process is one of the effective techniques that have been successfully employed for color removal from wastewater. Many adsorbents have been tested to reduce dye concentrations from aqueous solutions. Activated carbon is regarded as an effective but expensive adsorbent due to its high costs of manufacturing and regeneration [7,43]. Out of economic consideration, activated carbon is not used to treat a large quantity of effluents by a great scale of activated carbon. In addition to activated carbon, some adsorbents including peat [27,55], chitin [42], silica [45], perlite [17] and some agricultural wastes [48,49,56,63] have also been reported. However, the adsorption capacities of the above-mentioned adsorbents are not very high. In order to improve the efficiency of the adsorption processes, it is necessary to develop more cheap and easily available adsorbents with high adsorption capacities.

There is an increasing demand for porous materials as adsorbents and catalyst supports. Sepiolite, which is a zeolite-like clay mineral, provides a high specific surface area. Thus, it has many industrial applications as an adsorbent [11]. Sepiolite, which has a $(Si_{12})(Mg_8)O_{30}(OH)_4(OH_2)_4 \cdot 8H_2O$ unit-cell formula, is a magnesium hydrosilicate with a

* Corresponding author. Tel.: +90 266 249 3358; fax: +90 266 249 1012.
E-mail addresses: mdogan@balikesir.edu.tr (M. Doğan), yozdemir@balikesir.edu.tr (Y. Özdemir), malkan@balikesir.edu.tr (M. Alkan).

0143-7208/$ - see front matter © 2006 Elsevier Ltd. All rights reserved.
doi:10.1016/j.dyepig.2006.07.023

Nomenclature

K	Adsorption constant, L/g
q_e	Equilibrium dye concentration on adsorbent, mol/g
R^2	Linear regression coefficient
t	Time, s
T	Temperature, K
m	Mass of adsorbent, g
q_t	The amount of dye adsorbed per unit mass of the adsorbent at time, t, mol/g
C_0	Initial dye concentration in aqueous solution, mol/L
k_1	Adsorption rate constant for pseudo-first-order kinetic equation, s^{-1}
k_2	Adsorption rate constant for pseudo-second-order kinetic equation, g/mol min
$t_{1/2}$	The half-adsorption time of dye, s
k_i	Intra-particle diffusion rate constant, mol/$s^{1/2}$ g
β_L	Mass transfer coefficient, m/s
S_S	The surface area of adsorbent, m^2/g
C_t	Dye concentration in solution at time t, mol/L
r_0	The radius of the adsorbent particle, cm
D	Diffusion coefficient, cm^2/s
E_a	Activation energy, kJ/mol
R_g	Gas constant, J/K mol
k_0	Arrhenius factor, g/mol s
k_b	Boltzmann's constant
h	Planck's constant
ΔG^*	Free energy of activation, kJ/mol
ΔH^*	Enhalpy of activation, kJ/mol
ΔS^*	Entropy of activation, kJ/mol
β	The desorption constant, g/mol
α	The initial sorption rate, mol/g min

micro-fibrous structure and has a theoretical high surface area and high chemical and mechanical stability [24]. These characteristics of sepiolite are related to its powerful adsorbent properties and its ability to adsorb organic or inorganic ions. A general structure of sepiolite formed by alternation of blocks and tunnels that grow up in the microfibre direction. Each block consists of two tetrahedral silica sheets enclosing a central octahedral magnesia sheet but the silica sheets are discontinued and inversion of these sheets give rise to structural tunnels [22,57–60]. It owes much of its industrial applications to its molecular sized channels and large specific surface area (more than 200 m^2/g) [64]. Sepiolite is used in a variety of industries including cosmetics, ceramics, detergents, paper and paint. High-capacity values were also observed for heavy metal removal and wastewater treatment using sepiolite [11,59]. The abundance and availability of sepiolite reserves together with its relatively low cost guarantee its continued utilization.

Most of the world's sepiolite reserves are found in Turkey. Thus, it is important to characterize this clay mineral. Sorption depends heavily on experimental conditions such as initial dye concentration, ionic strength, pH and temperature [9,10]. Sepiolite has attracted remarkable attention by its sorptive, rheological and catalytic properties, and the use of sepiolitic clays is expanding [16,33,65]. The aim of this research is to investigate the adsorption kinetics of MV and MB on sepiolite from aqueous solutions. Therefore, the dynamical behaviors of adsorption were measured on the effect of contact time, stirring speed, ionic strength, pH and temperature. The adsorption rates were determined quantitatively and stimulated by the pseudo-first-order, the Elvoich and second-order models, and then adsorption mechanism was analyzed using intra-particle diffusion and mass transfer coefficient. Furthermore, thermodynamic activation parameters were also determined.

2. Material and methods

2.1. Materials

Sepiolite sample was obtained from Aktaş Lületaşı Co. (Eskişehir, Turkey). Some physical properties and the chemical composition of the sepiolite found in Eskişehir, Turkey are given in Tables 1 and 2; and some physicochemical properties of sepiolite in Table 3. In this study, MV and MB were chosen because of their known strong adsorptions onto solids. The adsorbate MV [C.I.: 42555, chemical formula: $C_{25}H_{30}N_3Cl$, MW: 393.96 g/mol, λ_{max}: 584 nm] and MB [C.I.: 52030, chemical formula: $C_{16}H_{18}N_3OS$, MW: 333.6 g/mol, λ_{max}: 663 nm] were supplied by Merck, Germany. The structures of MV and MB dyes are illustrated in Fig. 1a and b. Concentrations of dyes were determined by finding out the absorbance at the characteristic wavelength using a double beam UV–vis spectrophotometer (Cary 1E UV–visible spectrophotometer, Varian). Calibration curves were plotted between absorbance and concentration of the dye solution [4].

Sepiolite sample was treated before being used in the experiments as follows [2]: the suspension containing 10 g/L sepiolite was mechanically stirred for 24 h, and after waiting for about 2 min the supernatant suspension was filtered through filter paper. The solid sample was dried at 105 °C for 24 h, ground and then sieved using a 100 μm sieve. The particles under 100 μm were used in further experiments.

2.2. Adsorption kinetics

Dye solutions were prepared with distilled water. Since the dye is difficult to dissolve in water, the dye solution was allowed to stand for 1–2 days until the absorbance of the solutions remained unchanged. To study the effect of important

Table 1
Some physical properties of sepiolite [4]

Parameters	Data
Color	White
Melting temperature	1400–1450 °C
Drying temperature	40 °C
Reflective index	1.5

Table 2
The chemical composition of sepiolite [4]

Compounds	Weight (%)
SiO_2	53.47
MgO	23.55
CaO	0.71
Al_2O_3	0.19
Fe_2O_3	0.16
NiO	0.43
Weight loss	21.49

parameters like contact time, stirring speed, ionic strength, pH and temperature on the adsorptive removal of MV and MB dyes by sepiolite, experiments were conducted at 30 ± 1 °C. In systems, the dye concentration was 1.2×10^{-3} mol/L. The experiments of adsorption kinetics were carried out in a ca. 3-L stirred batch adsorber. For each experiment, 2.0 L of the basic dye solution at specified concentrations was continuously stirred at 400 rpm with 5 g of sepiolite. Samples were withdrawn at appropriate time intervals and then centrifuged at 4000 rpm for 15 min and the absorbance of the supernatant was measured. Experiments were carried out at solution pH. Effect of pH on dye removal was studied over a pH range of 5–9. pH was adjusted by the addition of dilute aqueous solutions of HCl or NaOH (0.10 M) by using a Orion 920A pH-meter with a combined pH electrode; and temperature was adjusted in the range of 20–50 °C. The pH-meter was standardized with NBS buffers before every measurement. A constant temperature bath was used to keep the temperature constant. Kinetics of adsorption was determined by analyzing adsorptive uptake of the dye from aqueous solution at different time intervals. The residual dye concentration was then determined. The adsorbed amounts of dyes were calculated from the concentrations in solutions before and after adsorption. Each experimental point was an average of two independent adsorption tests [3,18,19].

3. Results and discussion

3.1. Adsorption rate

Adsorption rate was investigated using the adsorbed dye concentrations at different stirring speeds, ionic strengths, pHs and temperatures as a function of time.

3.1.1. Effect of contact time

To determine the equilibration concentration and time, the adsorption of the cationic MV and MB dyes onto sepiolite was studied as a function of contact time. The contact time between adsorbate and the adsorbent is of significant importance in the wastewater treatment by adsorption. A rapid uptake of adsorbates and establishment of equilibrium in a short period signify the efficacy of that adsorbent for its use in wastewater treatment. In physical adsorption, most of the adsorbate species are adsorbed within a short interval of contact time. However, strong chemical binding of the adsorbate with adsorbent requires a longer contact time for the attainment of equilibrium. Available adsorption studies in literature reveal that the uptake of adsorbate species is fast at the initial stages of the contact period, and thereafter, it becomes slower near the equilibrium. In between these two stages of the uptake, the rate of adsorption is found to be nearly constant. This is obvious from the fact that a large number of vacant surface sites are available for adsorption during the initial stage, and after a lapse of time, the remaining vacant surface sites are difficult to be occupied due to repulsive forces between the solute molecules on the solid and bulk phases [40].

Table 3
Physicochemical properties of sepiolite

Parameters	Value	References
Surface area (m^2/g)	342	[4]
Density (g/cm)	2.5	[4]
Cation exchange capacity (meg/100 g)	25	[4]
pH of solution	7.8–8.3	[4]
Porosity	50.8%	[23]

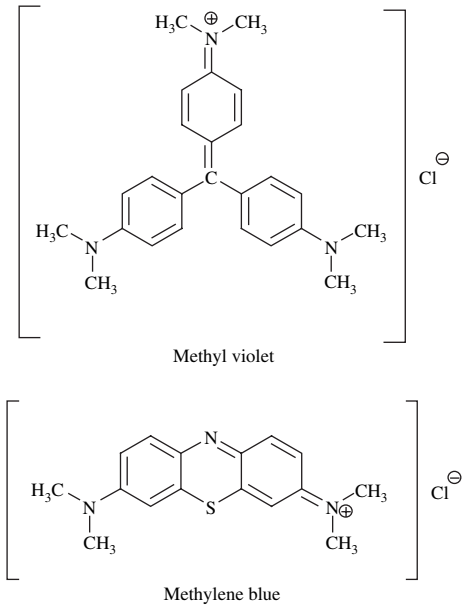

Fig. 1. The structures of dyes.

The effect of contact time on the adsorption of MV and MB dyes by sepiolite was studied for a period of 3 h (180 min) for initial dye concentration of 1.2×10^{-3} mol/L at 30 °C and solution pH. Sepiolite dosage was 2.5 g/L of dye solution for both MV and MB dyes. Dye solutions were kept in contact with sepiolite for 24 h although no significant variation in residual dye concentration was detected after 3 h of contact time. Thus, after 3 h of contact, a steady-state approximation was assumed and a quasi-equilibrium situation was accepted. Fig. 2 presents the effect of contact time for 3 h only. The contact time curve shows that the dye removal was rapid in the first 15 min. The curves of contact time are single, smooth and continuous leading to saturation. These curves indicate the possible monolayer coverage of dye on the surface of sepiolite [18,32,38,68].

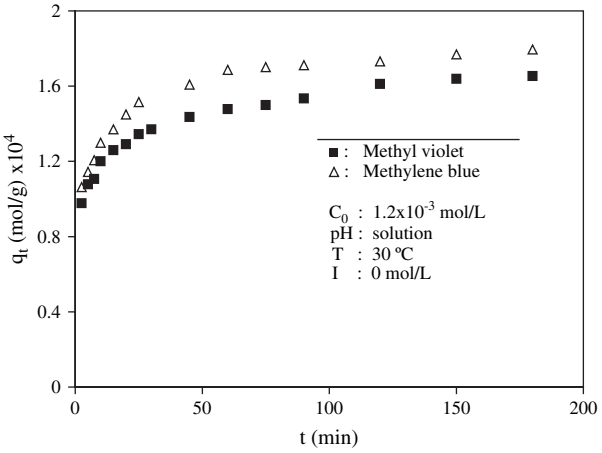

Fig. 2. The effect of contact time on the adsorption rate of dyes on sepiolite.

Pedro-Silva et al. [54] have reported 1 h equilibrium contact time for acid orange 7 dye adsorption on spent brewery grains. Similarly, a contact time of only about 25 min was required to attain the equilibrium adsorption of dyes to carbonaceous adsorbents [34]. Furthermore, we previously reported 30 min equilibrium contact time for removal of MV, MB and victoria blue by perlite at 30 °C [3,18,19]. As comparison, a quasi-equilibrium contact time of 3 h for MV and MB adsorption on sepiolite is much higher. We also found from Fig. 2 that the percent removal of MB was higher that of MV at any contact time. This trend was observed because methylene blue with smaller size could be adsorbed more deeply into that pore, which was big enough not to adsorb much greater size MV dye molecule.

3.1.2. Effect of stirring speed

Fig. 3a and b shows the experimental results obtained from a series of experiments performed, using different stirring speeds in the range of 200–600 rpm at 1.2×10^{-3} mol/L initial dye concentration, 30 °C and solution pH. As seen in Fig. 3a and b, it can be said that stirring speed had no significant effect on adsorption rate. Therefore, the stirring speed was taken as 400 rpm in further experiments.

3.1.3. Effect of ionic strength

There are a number of studies showing the changing of the removal order of dye with the concentration of various electrolyte types in dye medium. The effect of ionic strength on the adsorption rate of MV and MB on sepiolite was studied at 1×10^{-3}, 1×10^{-2}, and 1×10^{-1} mol/L NaCl concentrations at 30 °C and solution pH. As seen in Fig. 4, increasing ionic strength has significantly increased the adsorption rate of MV and MB on sepiolite. The presence of NaCl in the solution may have two opposite effects. On the one hand, since the salt screens the electrostatic interaction of opposite changes of the oxide surface and the dye molecules, the adsorbed amount should decrease with increase of NaCl concentration. On the other hand, the salt causes an increase in the degree of dissociation of the dye molecules by facilitating the protonation. The adsorbed amount increases as the dissociated dye ions

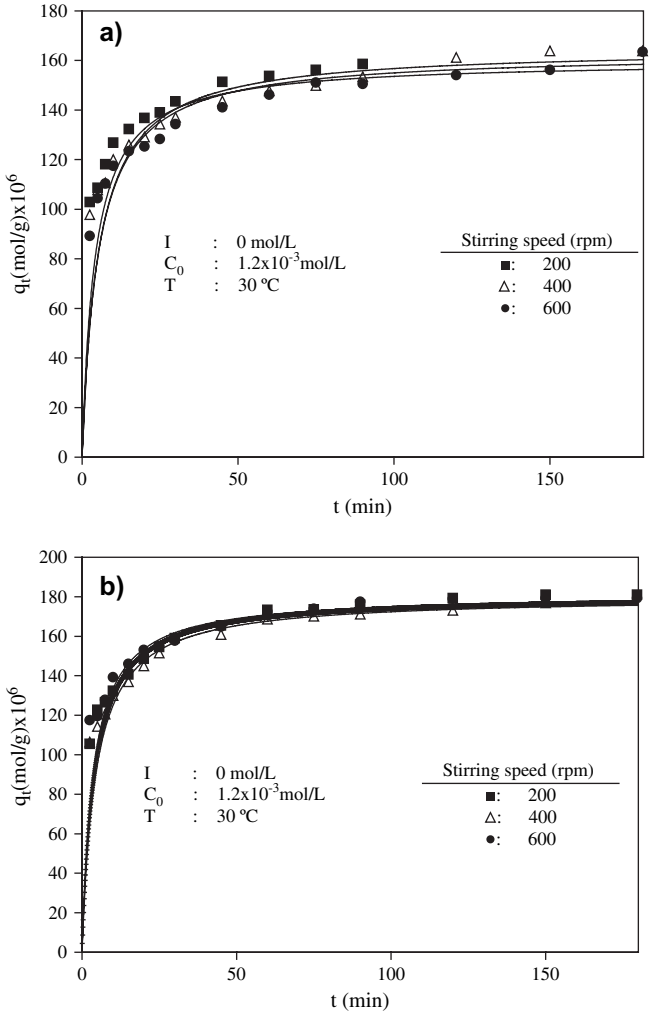

Fig. 3. The effect of stirring speed on the adsorption rate of (a) methyl violet and (b) methylene blue dyes on sepiolite.

free for binding electrostatically onto the solid surface of oppositely changed increase [13,62,66]. The latter effect seems to be dominant on the adsorption capacity of the surface.

3.1.4. Effect of pH

The pH of the solution affects the surface charge of the adsorbents as well as the degree of ionization of different pollutants. The hydrogen ion and hydroxyl ions are adsorbed quite strongly and therefore the adsorption of other ions is affected by the pH of the solution. Change of pH affects the adsorptive process through dissociation of functional groups on the adsorbent surface active sites. This subsequently leads to a shift in reaction kinetics and equilibrium characteristics of adsorption process. The adsorption of both MV and MB on sepiolite was studied in a pH range of 5–9 at 30 °C and the studies were carried out for 3 h. Initial dye concentration was 1.2×10^{-3} mol/L. Fig. 5 shows the effect of pH on the removal rate of MV and MB on sepiolite. The percentage removal of both MV and MB by sepiolite was increased with increase in pH. Alkan et al. [5] found that sepiolite had pH_{iep} at pH 6.6. In this case, sepiolite has negative zeta potential above

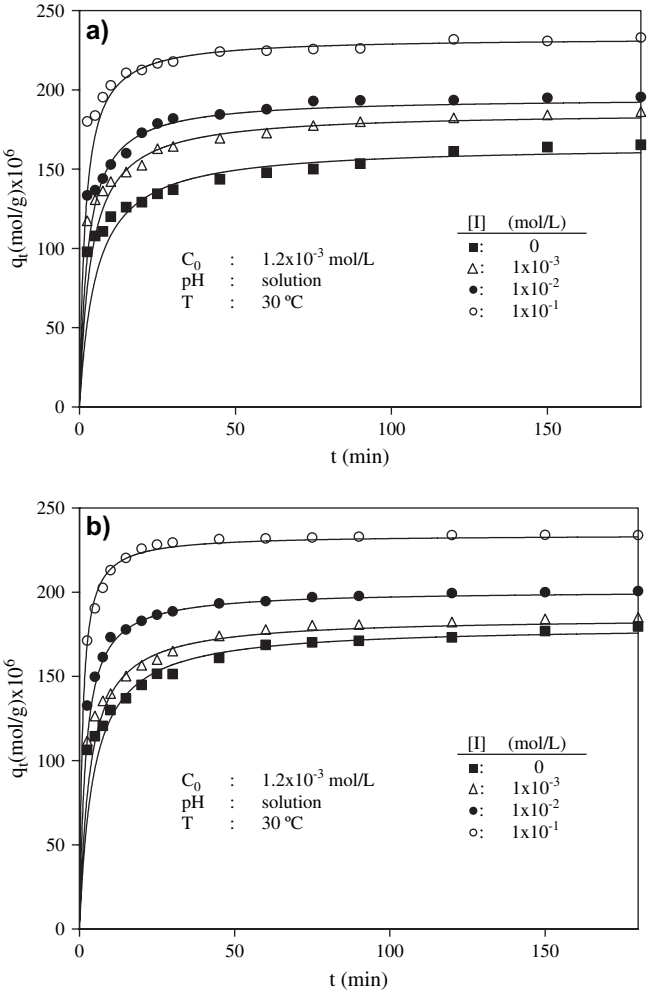

Fig. 4. The effect of ionic strength on the adsorption rate of (a) methyl violet and (b) methylene blue dyes on sepiolite.

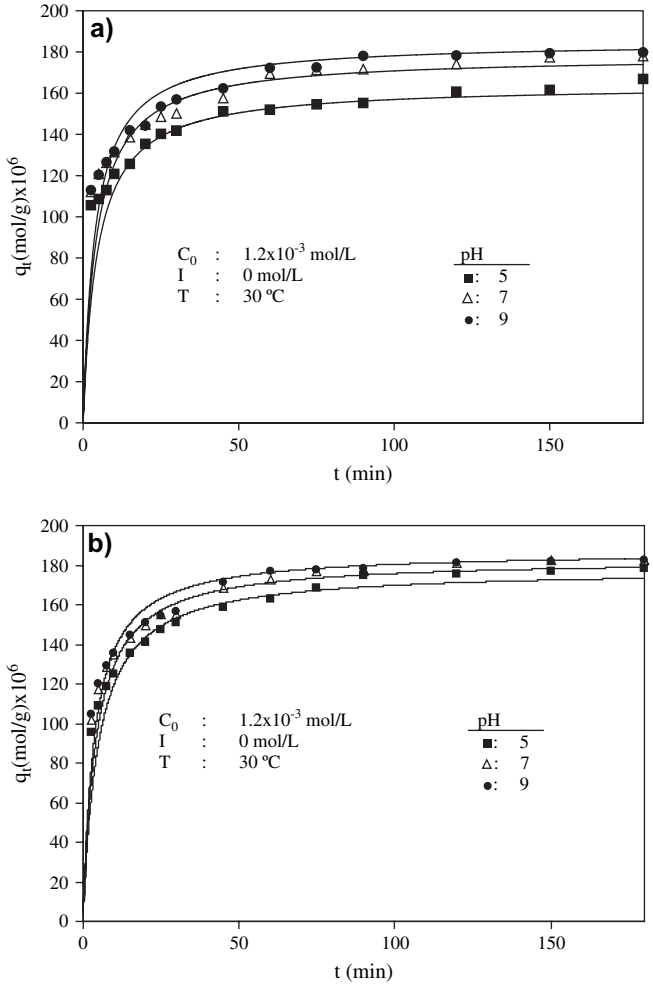

Fig. 5. The effect of pH on the adsorption rate of (a) methyl violet and (b) methylene blue dyes on sepiolite.

the value of pH_{iep}, and positive zeta potential below that of pH_{iep}. In this case, it can be said that the usage of higher pH from pH_{iep} for the adsorption of cationic dyes is fine. As the pH of the dye solutions becomes higher from pH_{iep}, the association of dye cations with negatively charged sepiolite surface can more easily take place as follows:

$$SO^- + Dye^+ = SO^-Dye^+ \quad (1)$$

According to Eq. (1), it can be said that the adsorption rate of MV and MB dyes on sepiolite increases with increase in solution pH. Higher removal of MV and MB in the alkaline pH range has been reported by other workers as well [18,19,39,40].

3.1.5. Effect of temperature

The effect of temperature on the adsorption rate of MV and MB on sepiolite was investigated at 20, 30, 40 and 50 °C. Increasing the temperature is known to increase the rate of diffusion of the adsorbate molecules across the external boundary layer and in the internal pores of the adsorbent particle, owing to the decrease in the viscosity of the solution. In addition, changing temperature will change the equilibrium capacity of the adsorbent for a particular adsorbate [8]. Fig. 6 shows the results of contact time experiments carried out at different temperatures for MV and MB adsorption on sepiolite. The removal of MV by adsorption on sepiolite increases from 1.56×10^{-4} mol/g to 1.76×10^{-4} mol/g when temperature of the solution is increased; and that of MB from 1.69×10^{-4} mol/g to 1.87×10^{-4} mol/g, indicating the process to be endothermic. This kind of temperature dependence of the adsorbed amount of the dyes may reflect the increase in the case with which the dye penetrates into the sepiolite because of its larger diffusion coefficient. In fact, a possible mechanism of interaction is the reaction between the hydroxyl endgroups of the sepiolite and the cationic group in the dye molecules; such a reaction could be favoured at higher temperatures [20].

3.2. Adsorption kinetics

It is important to be able to predict the rate at which contamination is removed from aqueous solutions in order to design an adsorption treatment plant. As seen in Figs. 3–6, the sorption processes are quite rapid and most of the dyes were retained within the first 3 h of contact. In order to investigate

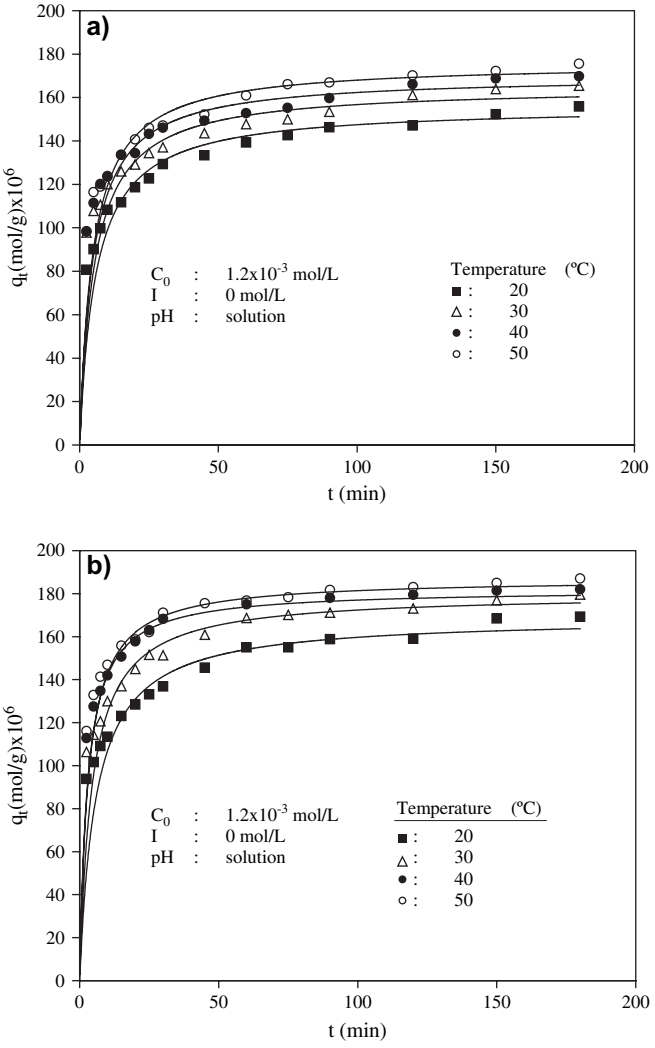

Fig. 6. The effect of temperature on the adsorption rate of (a) methyl violet and (b) methylene blue dyes on sepiolite.

the adsorption processes of MV and MB dyes on sepiolite, five kinetic models were used, including pseudo-first-order, the Elvoich equation, pseudo-second-order, mass transfer and intraparticle diffusion models. These models are most commonly used to describe the sorption of dyes as well as other pollutants (heavy metals) on solid sorbents [25,27–30,35,46,61] although, as pointed out by Ho and McKay [30], the application of a single kinetic model to the sorption on solid sorbents may be questionable because of the heterogeneity of the sorbent surfaces and diversity of sorption phenomena (transport, surface reactions). Parameters of the kinetic models were estimated from the experimental data with the aid of the nonlinear curve-fitting procedure.

3.2.1. Pseudo-first-order model

The pseudo-first-order kinetic model is more suitable for lower concentrations of solute. The pseudo-first-order [36] kinetic equation may be written in the form

$$\frac{dq_t}{dt} = k_1(q_e - q_t) \tag{2}$$

where q_t is the amount of adsorbate adsorbed at time t (mol/g); q_e is the adsorption capacity in equilibrium (mol/g); k_1 is the rate constant of pseudo-first-order model (min^{-1}); and t is the time (min). After definite integration by applying the initial conditions $q_t = 0$ at $t = 0$ and $q_t = q_t$ at $t = t$, the equation becomes [36]:

$$\ln(q_e - q_t) = \ln q_e - k_1 t \tag{3}$$

The plot of $\ln(q_e - q_t)$ against t should give a straight line with slope $-k_1$ and intercept $\ln q_e$. As seen in Tables 4 and 5, the correlation coefficient values for MV and MB adsorption on sepiolite have changed in the range of 0.908–0.980 and 0.854–0.988, respectively. These results have shown that the experimental data do not agree with the pseudo-first-order kinetic model.

Table 4
Kinetics data calculated for adsorption of MV on sepiolite

Parameters					Kinetics models							
					Pseudo-first-order model	Elvoich equation			Pseudo-second-order model			
T (°C)	$[C_0]$ (mol/L) $\times 10^3$	pH	Stirring speed (rpm)	$[I]$ (mol/L)	R^2	R^2	$\alpha \times 10^{-6}$	$\beta \times 10^5$	$q_{e(cal)}$ (mol/g) $\times 10^4$	$q_{e(exp)}$ (mol/g) $\times 10^4$	k_2 (g/mol min)	R^2
20	1.2	–	400	–	0.962	0.993	2.14	1.78	1.575	1.56	1109.28	0.998
30	1.2	–	400	–	0.970	0.996	9.01	1.63	1.677	1.65	1151.47	0.998
40	1.2	–	400	–	0.961	0.991	11.20	1.65	1.722	1.70	1244.18	0.998
50	1.2	–	400	–	0.970	0.990	5.89	1.81	1.778	1.76	1293.20	0.999
30	1.2	5	400	–	0.933	0.977	28.90	1.44	1.673	1.67	1352.81	0.999
30	1.2	7	400	–	0.961	0.992	17.20	1.68	1.812	1.78	1384.98	0.999
30	1.2	9	400	–	0.980	0.986	14.40	1.72	1.837	1.80	1405.28	0.999
30	1.2	–	200	–	0.975	0.992	13.30	1.62	1.716	1.70	1157.60	0.998
30	1.2	–	600	–	0.933	0.991	67.70	1.64	1.631	1.63	1189.15	0.998
30	1.2	–	400	0.001	0.960	0.993	26.10	1.69	1.880	1.88	1860.00	0.999
30	1.2	–	400	0.010	0.938	0.939	66.30	1.67	1.980	1.98	1950.00	0.999
30	1.2	–	400	0.100	0.908	0.950	574.60	1.27	2.330	2.33	2330.00	0.999

Table 5
Kinetics data calculated for adsorption of MB on sepiolite

Parameters					Kinetics models							
					Pseudo-first-order model	Elvoich equation			Pseudo-second-order model			
T (°C)	$[C_0]$ (mol/L) $\times 10^3$	pH	Stirring speed (rpm)	$[I]$ (mol/L)	R^2	R^2	$\alpha \times 10^{-6}$	$\beta \times 10^5$	$q_{e(cal)}$ (mol/g) $\times 10^4$	$q_{e(exp)}$ (mol/g) $\times 10^4$	k_2 (g/mol min)	R^2
20	1.2	–	400	–	0.875	0.991	2.55	1.88	1.72	1.69	1015.6	0.998
30	1.2	–	400	–	0.946	0.983	6.52	1.84	1.82	1.80	1256.2	0.999
40	1.2	–	400	–	0.575	0.954	36.20	1.63	1.84	1.82	1645.7	0.999
50	1.2	–	400	–	0.947	0.965	54.10	1.61	1.88	1.87	1929.6	0.999
30	1.2	5	400	–	0.981	0.988	2.41	2.03	1.82	1.78	1161.0	0.999
30	1.2	7	400	–	0.986	0.982	5.08	1.94	1.86	1.83	1321.6	0.999
30	1.2	9	400	–	0.972	0.976	7.07	1.88	1.86	1.82	1464.8	0.999
30	1.2	–	200	–	0.854	0.980	7.61	1.85	1.85	1.81	1387.5	0.999
30	1.2	–	600	–	0.968	0.973	23.00	1.67	1.84	1.81	1343.5	0.999
30	1.2	–	400	0.001	0.960	0.983	110.00	1.85	1.88	1.85	1632.9	0.999
30	1.2	–	400	0.010	0.938	0.903	473.00	1.49	2.02	2.01	2532.7	0.999
30	1.2	–	400	0.100	0.908	0.804	6200.00	1.30	2.35	2.34	4494.9	0.999

3.2.2. The Elovich equation

The Elovich equation is given as follows [47]:

$$\frac{dq_t}{dt} = \alpha \exp(-\beta q_t) \tag{4}$$

where α is the initial sorption rate (mol/g min) and β is the desorption constant (g/mol). To simplify the Elvoich equation, it is assumed that $\alpha\beta t \gg 1$ and by applying the boundary conditions $q_t = 0$ at $t = 0$, this equation becomes

$$q_t = \beta \ln(\alpha\beta) + \beta \ln t \tag{5}$$

Thus, the constants can be obtained from the slope and intercept of a straight line plot of q_t versus ln t. As seen in Tables 4 and 5, the correlation coefficients for the Elvoich equation have changed in the range of 0.939–0.996 and 0.804–0.991. This result has shown that the experimental data did not fit with the Elvoich equation.

3.2.3. Pseudo-second-order model

The rate of pseudo-second-order reaction is dependent on the amount of solute adsorbed on the surface of adsorbent and the amount adsorbed at equilibrium. The pseudo-second-order model can be represented in the following form [30]:

$$\frac{dq_t}{dt} = k_2(q_e - q_t)^2 \tag{6}$$

where k_2 is the rate constant of pseudo-second-order model (g/mol min). After integrating Eq. (6) for boundary conditions $q_t = 0$ at $t = 0$ and $q_t = q_t$ at $t = t$, the following form of equation can be obtained:

$$\frac{t}{q_t} = \frac{1}{k_2 q_e^2} + \frac{t}{q_e} \tag{7}$$

The pseudo-second-order rate constant (k_2) and the equilibrium adsorption capacity (q_e) can be determined experimentally from the slope and intercept of the plot of t/q_t versus t.

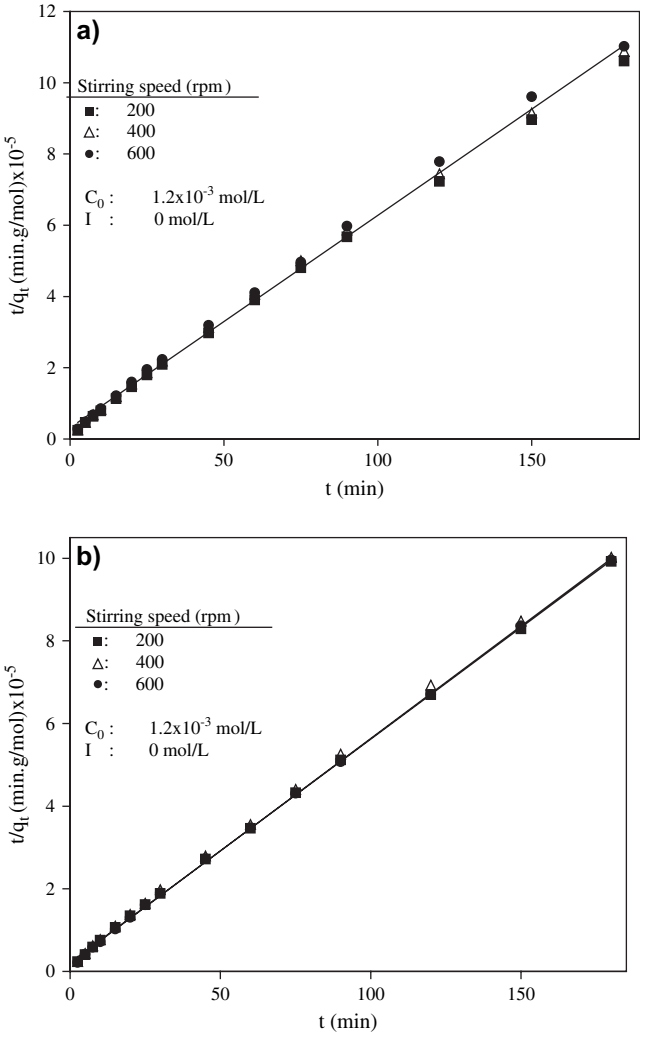

Fig. 7. The plots of t/q_t versus t for Fig. 3.

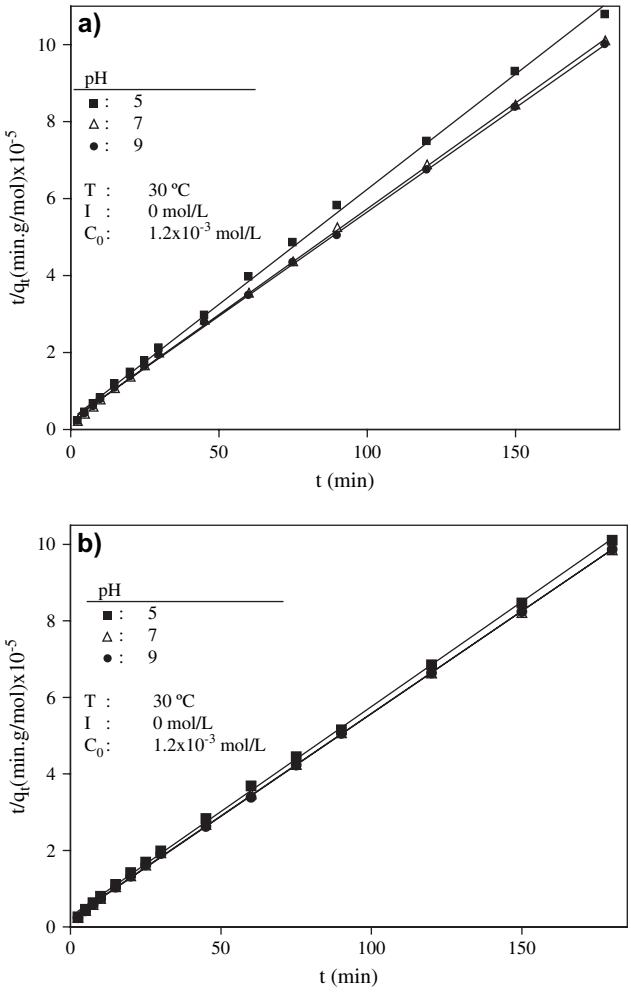

Fig. 8. The plots of t/q_t versus t for Fig. 4.

Figs. 7–10 show the plots of t/q_t versus t for the data of Figs. 3–6. Calculated correlation coefficients for pseudo-second-order model by using regression procedure for MV and MB adsorption are shown in Tables 4 and 5. Calculated correlation coefficients are closer to unity for pseudo-second-order kinetic model than the pseudo-first-order kinetic model and the Elvoich equation. Therefore, it was ascertained from a comparison of the predicted (best fitted) time dependencies with the experimental data that the pseudo-second-order kinetic equation describes the dye sorption more accurately, especially for longer time periods. The k_2 and q_e values calculated are listed in Tables 4 and 5. Similar phenomena have been observed in the biosorption of dye remazol black B on biomass [1], adsorption of congo red [49] and 2-chlorophenol [50] on coir pith carbon, and adsorption of MV, MB and victoria blue on perlite [3,18,19].

Half-adsorption time, $t_{1/2}$, is defined as the time required for the adsorption to take up half as much sepiolite as its equilibrium value. This time is often used as a measure of the adsorption rate

$$t_{1/2} = \frac{1}{k_2 q_e} \tag{8}$$

The values of $t_{1/2}$ determined for the tested parameters are given in Tables 4 and 5.

3.2.4. Adsorption mechanism

The adsorption mechanism for the removal of dyes may be assumed to involve the following three steps:

- Diffusion of the dye through the boundary layer,
- Intra-particle diffusion, and
- Adsorption of the dye on the sorbent surface.

The boundary layer resistance will be affected by the rate of adsorption and increase in contact time, which will reduce the resistance and increase the mobility of dye during adsorption. Since the uptake of dye at the active sites of sepiolite is a rapid process, the rate of adsorption is mainly governed by liquid phase mass transfer rate, diffusion through the boundary layer or intra-particle mass transfer rate [35].

3.2.4.1. Mass transfer coefficient. Mass transfer coefficient, β_L (m/s) of MV and MB at the sepiolite–solution interface, was determined by using Eq. (9) [12,52]:

$$\ln\left(\frac{C_t}{C_0} - \frac{1}{1+mK}\right) = \ln\left(\frac{mK}{1+mK}\right) - \left(\frac{1+mK}{mK}\right)\beta_L S_S t \tag{9}$$

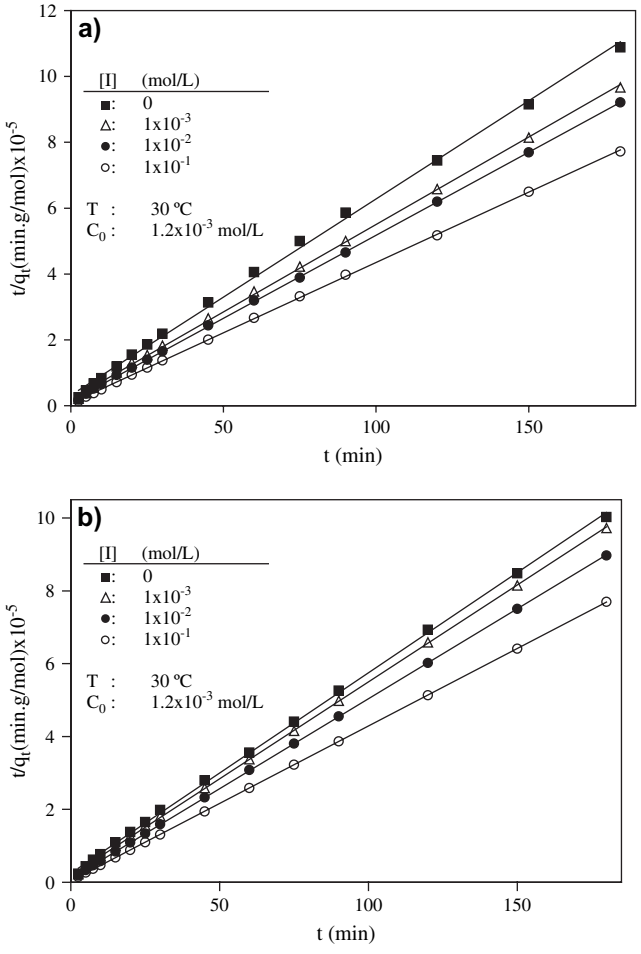

Fig. 9. The plots of t/q_t versus t for Fig. 5.

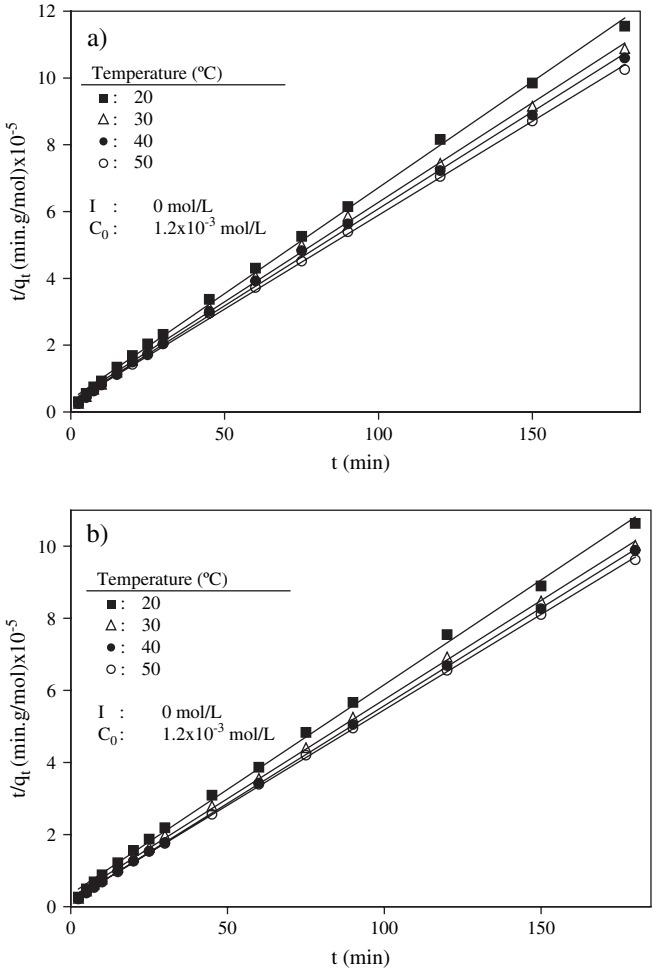

Fig. 10. The plots of t/q_t versus t for Fig. 6.

where K is the Langmuir constant (L/g); m is the mass of the adsorbent (g); and S_s is the surface area of adsorbent (m^2/g). A linear graphical relation of $\ln[(C_t/C_0)-1/(1+mK)]$ versus t was not obtained. In plotting the curves, K values for the adsorption of MV and MB onto sepiolite were taken from our previous work [53]. This result indicates that the model mentioned above for the system is not valid. The values of regression coefficient calculated from the equation mentioned above are given in Tables 6 and 7.

3.2.4.2. Intra-particle diffusion. The nature of the rate-limiting step in a batch system can also be assessed from the properties of the solute and adsorbent. Weber and Morris [67] stated that if intra-particle diffusion is the rate-controlling factor, uptake of the adsorbate varies with the square root of time. Thus, rates of adsorption are usually measured by determining the adsorption capacity of the adsorbent as a function of the square root of time [31]. Best-fit straight lines (plots are not shown) that do not pass through the origin indicate that there is an initial boundary layer resistance. An empirically found functional relationship, common to the most adsorption processes, is that the uptake varies almost proportionally with $t^{0.5}$, the Weber–Morris plot, rather than with the contact time, t [67]. The mathematical dependence of q_t versus $t^{0.5}$ is obtained if the sorption process is considered to be influenced by diffusion in the spherical particles and convective diffusion in the solution [6,41]. The root time dependence, known also as a Weber–Morris plot (1963), may be expressed by Eq. (10):

$$q_t = k_i\sqrt{t} + C \tag{10}$$

where k_i is a intra-particle diffusion rate parameter. According to Eq. (10), a plot of q_t versus $t^{0.5}$ should be a straight line with a slope k_i and intercept C when adsorption mechanism follows the intra-particle diffusion process. Values of intercept give an idea about the thickness of boundary layer, i.e., the larger the intercept the greater is the boundary layer effect [35]. The dependencies of q_t versus $t^{0.5}$ are only shown in Fig. 11 at different ionic strengths for the sorption of MV and MB (other figures not shown). As can be seen from Fig. 11, the plots of q_t against $t^{0.5}$ consist of two linear sections with different slopes. A similar multilinearity has been observed in other systems, e.g., for the dye sorption on sawdust [41], peat [21], or modified peat resin particles [61]. The multilinearity indicates that two or more steps occur in the sorption process. The two linear sections in the root time plots were evaluated separately

Table 6
Adsorption mechanism of MV on sepiolite

Parameters					Adsorption mechanism						$t_{1/2}$ (min)
T (°C)	$[C_0]$ (mol/L) × 10^3	pH	Stirring speed (rpm)	$[I]$ (mol/L)	Mass transfer R^2	Intra-particle diffusion					
						$k_{i,1} \times 10^7$	R^2	$k_{i,2} \times 10^8$	R^2	D ($cm^2/2$) × 10^{10}	
20	1.2	–	400	–	0.659	1.98	0.973	5.12	0.962	5.41	5.778
30	1.2	–	400	–	0.728	1.66	0.973	5.70	0.975	5.94	5.263
40	1.2	–	400	–	0.667	3.03	0.967	5.49	0.969	6.62	4.720
50	1.2	–	400	–	0.657	2.16	0.980	5.00	0.886	6.87	4.760
30	1.2	5	400	–	0.681	1.71	0.981	4.10	0.991	7.05	4.430
30	1.2	7	400	–	0.696	1.66	0.984	2.40	0.996	7.43	4.208
30	1.2	9	400	–	0.701	1.90	0.992	6.20	0.962	7.91	3.953
30	1.2	–	200	–	0.665	1.78	0.768	4.70	0.996	6.19	4.670
30	1.2	–	600	–	0.688	1.47	0.995	5.20	0.989	6.06	5.159
30	1.2	–	400	0.001	0.648	1.92	0.976	4.00	0.944	8.53	3.663
30	1.2	–	400	0.010	0.563	2.27	0.984	2.70	0.984	11.7	2.665
30	1.2	–	400	0.100	0.576	1.72	0.937	2.40	0.990	17.3	1.811

Table 7
Adsorption mechanism of MB on sepiolite

Parameters					Adsorption mechanisms						$t_{1/2}$ (min)
T (°C)	$[C_0]$ (mol/L) × 10^3	pH	Stirring speed (rpm)	$[I]$ (mol/L)	Mass transfer R^2	Intra-particle diffusion					
						$k_{i,1} \times 10^7$	R^2	$k_{i,2} \times 10^8$	R^2	D (cm^2/s) × 10^{10}	
20	1.2	–	400	–	0.707	1.86	0.991	6.80	0.990	5.37	5.82
30	1.2	–	400	–	0.646	2.23	0.994	3.20	0.993	7.07	4.42
40	1.2	–	400	–	0.407	2.46	0.993	2.20	0.990	11.10	2.82
50	1.2	–	400	–	0.570	1.75	0.995	2.90	0.998	12.10	3.09
30	1.2	5	400	–	0.624	2.29	0.987	3.40	0.977	6.46	4.84
30	1.2	7	400	–	0.600	1.94	0.995	1.89	0.982	7.57	4.13
30	1.2	9	400	–	0.590	1.89	0.985	1.80	0.998	8.33	3.75
30	1.2	–	200	–	0.628	1.94	0.997	2.90	0.990	7.85	3.98
30	1.2	–	600	–	0.632	2.04	0.994	2.40	0.998	7.73	3.58
30	1.2	–	400	0.001	0.578	1.94	0.990	1.90	0.992	9.44	3.31
30	1.2	–	400	0.010	0.460	2.40	0.992	2.40	0.992	15.90	1.96
30	1.2	–	400	0.100	0.350	1.42	0.982	9.00	0.988	32.90	0.95

using Eq. (10), and the model parameters are listed in Tables 6 and 7. The first straight portion is attributed to the macro-pore diffusion (phase I) and the second linear portion to micro-pore diffusion (phase II) [6]. In the first section, the diffusion rate parameters $k_{i,1}$ vary with the dye concentration. In the second section, the diffusion rate parameters do not exhibit a distinct dependence on the dye concentration. In phase (I), about 75–80% of both MV and MB was taken up by sepiolite within a $t^{0.5}$ value of 4 min. This is attributed to the instantaneous utilization of the most readily available adsorbing sites on the adsorbent surface. Phase (II) may be attributed to a very slow diffusion of the adsorbates from the surface film into the micro-pores, which are the least accessible sites of adsorption. This also stimulates a very slow rate of migration of adsorbates from the liquid phase on to the adsorbent surface. The values of $k_{i,1}$ and $k_{i,2}$ obtained from the slopes of straight lines are listed in Tables 6 and 7. A comparison between the reaction orders and adsorption mechanisms of sepiolite and other adsorbents is presented in Table 8. Similar results were found for basic red 22 on pith [27] and methylene blue on perlite [19].

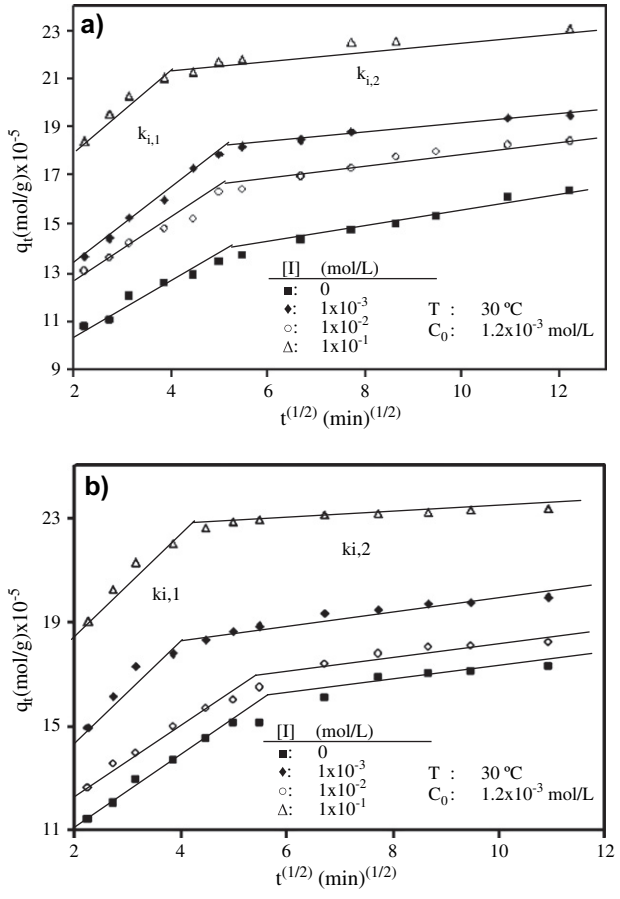

Fig. 11. Intra-particle diffusion plots for different ionic strengths: (a) methyl violet and (b) methylene blue.

3.3. Diffusion coefficient

The values of diffusion coefficient largely depend on the surface properties of adsorbents. The diffusion coefficients for the intra-particle transport of MV and MB within the pores of sepiolite particles have been calculated at different concentrations, ionic strengths, pHs and temperatures by employing Eq. (11).

$$t_{1/2} = \frac{0.030 r_0^2}{D} \tag{11}$$

where D is the diffusion coefficient with unit cm^2/s; $t_{1/2}$ is the time (s) for half-adsorption of MV and MB and r_0 is the radius of the adsorbent particle in cm. The value of r_0 was calculated as 2.5×10^{-3} cm for sepiolite sample. In these calculations, it has been assumed that the solid phase consists of spherical particles with an average radius between the radii corresponding to upper- and lower-size fractions. For the present study, the pore diffusion coefficient values obtained from Eq. (11) are given in Tables 6 and 7. The values of diffusion coefficient for adsorption of MV increase from 5.4×10^{-10} cm^2/s to 6.87×10^{-10} cm^2/s with change in temperature from 20 to 50 °C, and those for adsorption of MB from

Table 8
Adsorption order and mechanism of some dyes on various adsorbents

Adsorbents	Reaction order	Adsorbates	Adsorption mechanism	References
Activated carbon	First order	Methylene blue	Intra-particle diffusion	[35]
Pith	Pseudo-second-order	Basic red 22	Intra-particle diffusion	[27]
Wood	–	Astrazon blue	Intra-particle diffusion	[41]
Perlit	Second order	Methylene blue	Intra-particle diffusion	[19]
Perlit	First order	Methyl violet	Intra-particle diffusion	[18]
Perlit	First order	Victoria blue	–	[3]
Modified peat–resin particle	–	Basic Magenta and Basic Brilliant Green	Intra-particle diffusion	[61]

5.37×10^{-10} cm^2/s to 12.1×10^{-10} cm^2/s. These results agree with those of Haimour and Sayed, McKay and Allen, and Al-qodah [8,26,44] . Compared to benzene derivatives on carbon and astrazone blue and telon blue on wood [44], the D values for MV and MB adsorption on sepiolite are much lower than those of benzene derivatives. The D values of phenol and benzene on carbon are 901×10^{-10} and 80×10^{-10} cm^2/s, respectively. This was attributed to the larger molecular size of the present systems, the factor that slows down in diffusion rate. In addition, the present molecules have more complex structures than benzene derivatives, and therefore its strong interaction nature with sepiolite surface reduces its mobility. Furthermore, the diffusion coefficient values, D, for MV and MB adsorption on sepiolite are higher than those for astrazone blue and telon blue on wood [41]. The diffusion coefficients vary from 6.0×10^{-13} to 1.8×10^{-13} cm^2/s for astrazone blue and from 3.0×10^{-13} to 8.0×10^{-13} cm^2/s for telon blue.

3.4. Activation parameters

The second-order rate constants listed in Tables 4 and 5 have been used to estimate the activation energy of MV and MB adsorption on sepiolite using Arrhenius equation:

$$\ln k_2 = \ln k_0 - \frac{E_a}{R_g T} \tag{12}$$

where E_a is activation energy (J/mol); k_2 is the rate constant of sorption (g/mol s); k_0 is Arrhenius factor, which is the temperature independent factor (g/mol s); R_g is the gas constant (J/K mol); and T is the solution temperature (K). The slope of plot of $\ln k_2$ versus $1/T$ is used to evaluate E_a, which was found to be 4.2 kJ/mol and 17.3 kJ/mol for MV and MB adsorption, respectively. Fig. 12 shows the plots of $\ln k_2$ versus $1/T$ for both dyes. These values are consistent with the values in the literature where the activation energy was found to be 43.0 kJ/mol for the adsorption of reactive red 189 on cross-linked chitosan beads [15], or 5.6–49.1 kJ/mol for the adsorption of polychlorinated biphenyls on fly ash [51]. The second-order rate constants have increased with the increase in temperature. As known when the rate is controlled by intra-particle diffusion mechanism, the activation energy is very low and hence it can be concluded that the process is governed by interactions of physical nature [19].

Free energy (ΔG^*), enthalpy (ΔH^*) and entropy (ΔS^*) of activation can be calculated by Eyring equation [37]:

$$\ln\left(\frac{k_2}{T}\right) = \ln\left(\frac{k_b}{h}\right) + \frac{\Delta S^*}{R_g} - \frac{\Delta H^*}{R_g T} \tag{13}$$

where k_b and h are Boltzmann's and Planck's constants, respectively. According to Eq. (13), a plot of $\ln(k_2/T)$ versus $1/T$ should be a straight line with a slope $-\Delta H^*/R_g$ and intercept $[\ln(k_b/h) + \Delta S^*/R_g]$. ΔH^* and ΔS^* were calculated from slope and intercept of line, respectively (Fig. 13). Gibbs energy of activation may be written in terms of entropy and enthalpy of activation:

$$\Delta G^* = \Delta H^* - T\Delta S^* \tag{14}$$

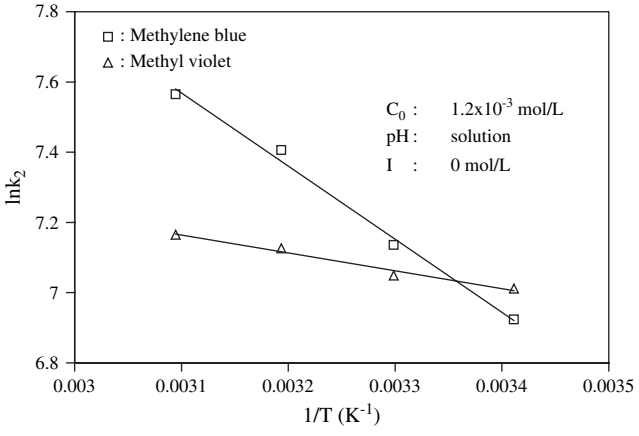

Fig. 12. Arrhenius plots for adsorption of dyes on sepiolite.

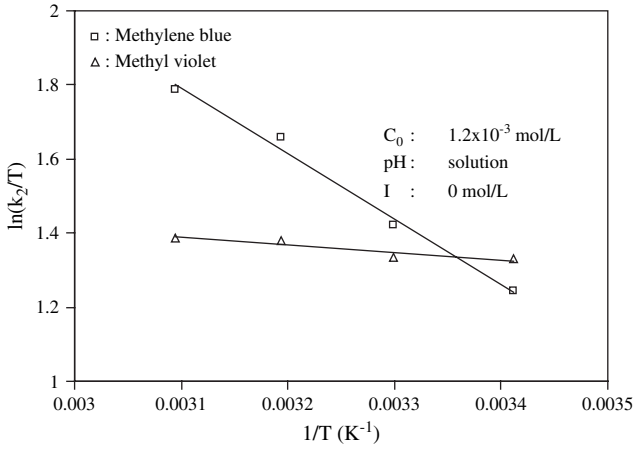

Fig. 13. Plots of $\ln(k_2/T)$ versus $1/T$ for adsorption of dyes on sepiolite.

ΔG^* was calculated at 293 K from Eq. (14). It is found that the values of the free energy (ΔG^*), enthalpy (ΔH^*) and entropy (ΔS) of activation for MV and MB are 52.9 kJ/mol, 1.8 kJ/mol and −174.5 J/mol K, and 53.1 kJ/mol, 14.8 kJ/mol and −130.6 J/mol K, respectively. The fact that the activation entropy is negative is a result of interactions between dyes and sepiolite as expected.

3.5. Conclusions

We investigated the adsorption kinetics of MV and MB dyes on sepiolite as a function of contact time, stirring speed, initial dye concentration, ionic strength, pH and temperature; and found that (i) the adsorption rate of dyes on sepiolite increased with increase in initial dye concentration, ionic strength, pH and temperature but stirring speed had no effect on it; (ii) the intra-particle diffusion was the rate-limiting step for the adsorption process; (iii) the diffusion coefficient increased with increase in the initial dye concentration, ionic strength, pH and temperature; and (iv) the activation energy was very low and the process is governed by interactions of physical nature. Sepiolite can be used for the removal of cationic dyes from aqueous solutions.

Acknowledgements

The authors thank the Balikesir University Research Center of Applied Science (BURCAS).

References

[1] Aksu Z, Tezer S. Equilibrium and kinetic modelling of biosorption of Remazol Black B by *Rhizopus arrhizus* in a batch system: effect of temperature. Process Biochem 2000;36:431–9.
[2] Alkan M, Doğan M. Adsorption of copper (II) onto perlite. J Colloid Interface Sci 2001;243:280–91.
[3] Alkan M, Doğan M. Adsorption kinetics of victoria blue onto perlite. Fresenius Environ Bull 2003;12(5):418–25.
[4] Alkan M, Çelikçapa S, Demirbaş Ö, Doğan M. Removal of reactive blue 221 and acid blue 62 anionic dyes from aqueous solutions by sepiolite. Dyes Pigments 2005a;65(3):251–9.
[5] Alkan M, Demirbaş Ö, Doğan M. Electrokinetic properties of sepiolite suspensions in different electrolyte media. J Colloid Interface Sci 2005b;281(1):240–8.
[6] Allen SJ, McKay G, Khader KYH. Intraparticle diffusion of a basic dye during adsorption onto sphagnum peat. Environ Pollut 1989;56:39.
[7] Allen SJ. Types of adsorbent materials. In: McKay G, editor. Use of adsorbents for the removal of pollutants from wastewaters. Boca Raton: CRC, Inc.; 1996. p. 59.
[8] Al-qodah Z. Adsorption of dyes using shale oil ash. Water Res 2000;34(17):4295–303.
[9] Bailey SE, Olin TJ, Bricka RM, Adrian D. A review of potentially low cost sorbents for heavy metals. Water Res 1999;33(11):2469–79.
[10] Balci S. Effect of heating and acid pre-treatment on pore size distribution of sepiolite. Clay Miner 1999;34:647–55.
[11] Balci S, Dincel Y. Ammonium ion adsorption with sepiolite: use of transient uptake method. Chem Eng Process 2002;41:79–85.
[12] Batabyal D, Sahu A, Chaudhuri SK. Kinetics and mechanism of removal of 2,4-dimethyl phenol from aqueous solutions with coal fly ash. Sep Sci Technol 1995;5(4):179–86.
[13] Blockhaus F, Sequaris JM, Narres HD, Schwuger MJ. Adsorption–desorption behavior of acrylic–maleic acid copolymer at clay minerals. J Colloid Interface Sci 1997;186:234–47.
[14] Chiou MS, Ho PY, Li HY. Adsorption behavior of dye AAVN and RB4 in acid solutions on chemically cross-linked chitosan beads. J Chin Inst Chem Eng 2003;34(6):625–34.
[15] Chiou MS, Li HY. Adsorption behavior of reactive dye in aqueous solution on chemical cross-linked chitosan beads. Chemosphere 2003;50:1095–105.
[16] Daza L, Mendioroz S, Pajares JA. Mercury adsorption by sulfurized fibrous silicates. Clays Clay Miner 1991;39(1):14–21.
[17] Doğan M, Alkan M, Onganer Y. Adsorption of methylene blue on perlite from aqueous solutions. Water Air Soil Pollut 2000;120:229–48.
[18] Doğan M, Alkan M. Adsorption kinetics of methyl violet onto perlite. Chemosphere 2003;50:517–28.
[19] Doğan M, Alkan M, Türkyılmaz A, Özdemir Y. Kinetics and mechanism of removal of methylene blue by adsorption onto perlite. J Hazard Mater 2004;B109:141–8.
[20] Espinosa-Jiménez M, Perea-Carpio R, Padilla-Weigand R, Ontiversos A. Electrokinetic and thermodynamic analysis of the dyeing process of polyamide fabric with mordant black 17. J Colloid Interface Sci 2001;238:33–6.
[21] Furusawa T, Smith JM. Mass-transfer rates in slurries by chromatography. Ind Eng Chem Fundam 1973;12(3):360–4.
[22] Gonzales-Pradas E, Villafranca-Sanchez M, Socias-Viciana M, Fernandez-Perez M, Urena-Amate MD. Preliminary studies in removing atrazine, isoproturon and imidacloprid from water by natural sepiolite. J Chem Technol Biotechnol 1999;74(5):417–22.
[23] Göktaş AA, Misirli Z, Baykara T. Ceram Int 1997;23:305–11.
[24] Grim RE. Clay mineralogy. New York: McGraw Hill; 1968.
[25] Gupta VK, Srivastava SK, Mohan D. Equilibrium uptake, sorption dynamics, process optimization, and column operations for the removal and recovery of malachite green from wastewater using activated carbon and activated slag. Ind Eng Chem Res 1997;36(6):2207–18.
[26] Haimour N, Sayed S. Natural Eng Sci 1997;24(2):215–24.
[27] Ho YS, McKay G. Sorption of dye from aqueous solution by peat. Chem Eng J 1998a;70:115.
[28] Ho YS, McKay G. The kinetics of sorption of basic dyes from aqueous solution by sphagnum moss peat. Can J Chem Eng 1998b;76(4):822–7.
[29] Ho YS, McKay G. Kinetic models for the sorption of dye from aqueous solution by wood. Proc Saf Environ Protect 1998c;76(B2):183–91.
[30] Ho YS, McKay G. Pseudo-second order model for sorption processes. Process Biochem 1999;34:451–65.
[31] Ho YS, McKay G. Sorption of dyes and copper ions onto biosorbents. Process Biochem 2003;38(7):1047–61.
[32] Inbraj BS, Sulochana N. Basic dye adsorption on a low cost carbonaceous sorbent – kinetic and equilibrium studies. Indian J Technol 2002;9:201–8.
[33] Inegahi S, Fukushima Y, Doi H, Kamigaito O. Pore-size distribution and adsorption selectivity of sepiolite. Clay Miner 1990;25:99–105.
[34] Jain AK, Gupta VK, Bhatnagar A, Suhas. A comparative study of adsorbents prepared from industrial wastes for removal of dyes. Sep Sci Technol 2003;38:463–81.
[35] Kannan N, Sundaram M. Kinetics and mechanism of removal of methylene blue by adsorption on various carbons—a comparative study. Dyes Pigments 2001;51:25–40.
[36] Lagergren S. About the theory of so called adsorption of soluble substances. K Svenska Vetenskapsad Handl 1898;24:1–6.
[37] Laidler KJ, Meiser JH. Physical chemistry. New York: Houghton Mifflin; 1999. p. 852.
[38] Malik PK. Use of activated carbons prepared from sawdust and rice-husk for adsorption of acid dyes: a case study of acid yellow 36. Dyes Pigments 2003;56:239–49.
[39] Mall ID, Upadhyay SN. Treatment of methyl violet bearing wastewater from paper mill effluent using low cost adsorbents. J Indian Pulp Paper Technol Assoc 1995;7(1):51–7.

[40] Mall ID, Srivastava VC, Agarwal NK. Removal of Orange-G and Methyl Violet dyes by adsorption onto bagasse fly ash—kinetic study and equilibrium isotherm analyses. Dyes Pigments 2006;69:210–23.
[41] McKay G, Poots VJP. Kinetics and diffusion processes in colour removal from effluent using wood as an adsorbent. J Chem Technol Biotechnol 1980;30:279–92.
[42] McKay G, Blair HS, Gardner JR. Rate studies for the adsorption of dyestuffs on chitin. J Colloid Interface Sci 1983;95:108.
[43] McKay G. The adsorption of dyestuffs from aqueous solution using activated carbon: analytical solution for batch adsorption based on external mass transfer and pore diffusion. Chem Eng J 1983;27:187.
[44] McKay G, Allen SJ. Single resistance mass transfer models for the adsorption of dyes on peat. J Sep Process Technol 1983;4(3):1–7.
[45] McKay G. Analytical solution using a pore diffusion model for a pseudo-irreversible isotherm for the adsorption of basic dye on silica. AIChE J 1984;30:692.
[46] McKay G. AIChE J 1985;31:335.
[47] McKay G, Ho YS, Ng JCY. Bisorption of copper from waste waters: a review. Sep Purif Methods 1999;28:87–125.
[48] Namasivayam C, Prabha D, Kumutha M. Removal of direct red and acid brilliant blue by adsorption on to banana pith. Bioresour Technol 1988; 64:77.
[49] Namasivayam C, Kavitha D. Removal of congo red from water by adsorption onto activated carbon prepared from coir pith, an agricultural solid waste. Dyes Pigments 2002;54:47–8.
[50] Namasivayam C, Kavitha D. Adsorptive removal of 2-chlorophenol by low-cost coir pith carbon. J Hazard Mater 2003;B98:257–74.
[51] Nollet H, Roels M, Lutgen P, Van der Meeren P, Verstraete W. Removal of PCBs from wastewater using fly ash. Chemosphere 2003;53:655–65.
[52] Onganer Y, Temur Ç. Adsorption dynamics of Fe (III) from aqueous solutions onto activated carbon. J Colloid Interface Sci 1998;205(2):241–4.
[53] Özdemir Y. MSc thesis, Balıkesir University, Department of Chemistry, Balıkesir, Turkey; 2005 [in Turkish].
[54] Pedro-Silva J, Sousa S, Rodrigues J, Antunes H, Porter JJ, Goncalves I, et al. Adsorption of acid orange 7 dye in aqueous solutions by spent brewery grains. Sep Purif Technol 2004;40:309–15.
[55] Ramakrishna KR, Viraraghavan T. Dye removal using low cost adsorbents. Water Sci Technol 1997;36:189.
[56] Robinson T, Chandran P, Nigam P. Removal of dyes from a synthetic textile dye effluent by biosorption on apple pomace and wheat straw. Water Res 2002;36:2824.
[57] Rytwo G, Nir S, Serban C, Margulies L, Casal B, Merino L, et al. Adsorption of monovalent organic cations on sepiolite: experimental results and model calculations. Clays Clay Miner 1998;46(3):340–8.
[58] Rytwo G, Tropp D, Serban C. Adsorption of diquat, paraquat and methyl green on sepiolite: experimental results and model calculations. Appl Clay Sci 2002;20(6):273–82.
[59] Sabah E, Celik MS. Adsorption mechanism of quaternary amines by sepiolite. Sep Sci Technol 2002;37(13):3081–97.
[60] Sabah E, Turan M, Celik MS. Adsorption mechanism of cationic surfactants onto acid- and heat-activated sepiolites. Water Res 2002;36(16): 3957–64.
[61] Sun Q, Yang L. The adsorption of basic dyes from aqueous solution on modified peat–resin particle. Water Res 2003;37(7):1535–44.
[62] Tekin N, Demirbaş Ö, Alkan M. Adsorption of cationic polyacrylamide onto kaolinite. Microporous Mesoporous Mater 2005;85(3): 340–50.
[63] Tsai WT, Chang CY, Lin MC, Chien SF, Sun HF, Hsieh MF. Adsorption of acid dye onto activated carbon prepared from agricultural waste bagasse by $ZnCl_2$ activation. Chemosphere 2001;45:51.
[64] Türker AR, Bag H, Erdogan B. Determination of iron and lead by flame atomic absorption spectrometry after preconcentration with sepiolite. Fresenius J Anal Chem 1997;357:351–3.
[65] Unal HI, Erdogan B. The use of sepiolite for decolorization of sugar juice. Appl Clay Sci 1998;12:419–29.
[66] Vermöhlen K, Lewandowski H, Narres HD, Schwuger MJ. Adsorption of polyelectrolytes onto oxides – the influence of ionic strength, molar mass, and Ca2+ ions. Colloids Surf A 2000;163:45–53.
[67] Weber WJ, Morris JC. Kinetics of adsorption on carbon from solution. J Sanit Eng Div ASCE 1963;89(SA2):31–59.
[68] Wong Y, Yu J. Laccase catalysed decolorisation of synthetic dyes. Water Res 1999;33(16):3512–20.